2007 IEEE International Conference on
Robotics and Automation
Roma, Italy, 10-14 April 2007

Differentially Flat Design of Bipeds Ensuring Limit-Cycles

Vivek Sangwan and Sunil K. Agrawal

***Abstract*— In bipedal walking, a trajectory is acceptable as long as it is repetitive and allows the foot to clear the ground, while allowing the biped to move forward. Since the actual trajectory followed by a biped is not as important, a biped having more than one passive joints can also meet the motion requirements. Due to physical constraints, a biped is under-actuated at the ground contact with the feet. A biped should exhibit limit cycles when moving continuously in an environment. In general, it is difficult to prove existence of limit cycles for nonlinear systems. In this work, we generate limit cycles for a class of nonlinear under-actuated bipeds using differential flatness. A specific inertia distribution renders the biped design differentially flat. Differential Flatness allows generation of a family of limit cycles amenable to numerical optimization. The results are illustrated by two DOF biped.**

I. INTRODUCTION

Bipedal locomotion is a problem that has been studied for a couple of decades now, but still is far from being fully solved. Bipedal robots are hard to control due to highly nonlinear dynamics, under-actuation, impacts and change in the structure of system across impacts. In biped walking, strictly following a predefined trajectory is not critical. Instead, criterion such as periodicity, ground clearance of the swinging leg and the approximate shape of the trajectories are important. Since a biped is not required to follow any particular set of joint trajectories, it is not absolutely essential to have an actuator at each joint. From natural constraints, there can not be an actuator between the foot and the ground. In the phase, where the foot is not flat on the ground, but is rolling along the edge, it is under-actuated. These facts imply that studying bipeds as nonlinear under-actuated systems can add to the understanding of bipedal locomotion and control.

There can be three categories of a mechanical system based on the number of actuators present compared to the number of degrees-of-freedom: Fully actuated, Under-actuated and completely Passive. One of the early attempts for bipeds to walk purely under gravity, without actuation, was by McGeer [1], who demonstrated that a planar robot can walk down a shallow slope without any actuation. A three dimensional analog of planar gravity powered robot has also been demonstrated [2]. The fully actuated robots, such as Honda humanoid robots [3] and Japanese HRP-2P [4] are on the other extreme. Whereas passive robots require no elaborate control system, actively controlled robots need very complex controllers. On one hand, completely passive bipeds do not consume any energy but the modulation of motion is limited. On the other hand, fully active bipeds control elaborately the motion but at the expense of complexity and energy. In between these two extremes is the class of under-actuated bipeds. Previous works on under-actuated bipeds include [5], [6], [7], [8]. The most critical requirement for any system to be used as a biped is existence of limit cycles. A fully actuated system can be made to go through any trajectory but for a nonlinear under-actuated system it is difficult to analytically prove the existence of limit cycles.

The technical approach adopted in this paper is to investigate the property of *differential flatness* [9], [10], [11] for under-actuated planar bipeds. In general, for an under-actuated system, not all outputs can be controlled arbitrarily. The paradigm of differential flatness allows the determination of those outputs that can be controlled arbitrarily for an under-actuated system, called the flat outputs. The number of these outputs equals the number of inputs. Also, differential flatness provides a transformation between these flat outputs and the system states and inputs, a diffeomorphism. Once this property is established, trajectory between any two points in its differentially flat output space is feasible and can be shown to be consistent with the dynamics of the under-actuated system. *Input-state feedback linearizable* systems are a subclass of differentially flat systems. In this paper, we show that certain choices of inertia distributions make an under-actuated open-chain planar biped with revolute joints feedback linearizable, i.e., also differentially flat. Hence, cyclic trajectories can be guaranteed for these under-actuated bipeds. A similar study for planar under-actuated open chain linkages has been presented in [12].

The key contributions of this paper are as follows: (i) Identification of a class of under-actuated nonlinear differentially flat bipeds, (ii) Generation and tracking of limit-cycles for the above-mentioned class of under-actuated bipeds (iii) Presentation of a fabricated prototype of the biped.

The rest of the paper is organized as follows: Section II describes the class of differentially flat under-actuated bipeds. The general procedure for the planning and tracking of limit-cycles for these systems is presented in Section III. Specific results for a two DOF biped are presented in sections IV. Details of a fabricated prototype are presented in section V. Finally, conclusions are presented in Section VI.

II. DYNAMIC DESIGN OF DIFFERENTIALLY FLAT BIPEDS

A planar biped having arbitrary number of segments in each of its leg is shown in Fig. 1. It does not have feet and the ground contact is considered to be revolute. The

Vivek Sangwan is a PhD student at Department of Mechanical Engineering, Mechanical Systems Lab, University of Delaware, DE, USA sangwan@udel.edu

Sunil K. Agrawal is a Professor at Department of Mechanical Engineering, , Mechanical Systems Lab, University of Delaware, DE, USA agrawal@me.udel.edu

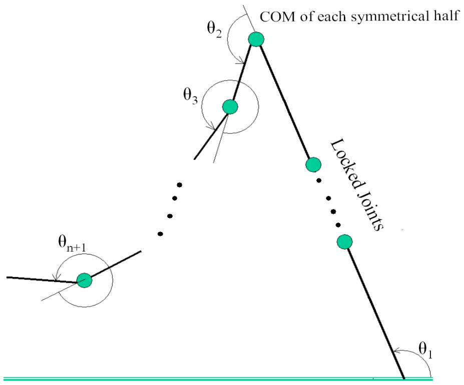

Fig. 1. An n-DOF planar biped robot. Each leg is identical having $(n-1)$ links, making a total of $2(n-1)$ links. All joints in stance leg are locked reducing the effective number of links at any given time instant to n, furthermore, some or all joints in the swing can get locked after impacts, like the knee impact to avoid hyper-extension.

walking cycle consists of single support phases separated by instantaneous impacts. It is assumed that both legs are identical and all the joints in the stance leg are locked. This general structure resembles an n degree-of-freedom planar open chain manipulator, with the stance leg as the first link and all other moving links present in the swing leg. For an n degree-of-freedom open-chain robot described by the coordinates q_1,q_2,...,q_n, the structure of the dynamic equations [13] is given by

$$A(q)\ddot{q} + b(q,\dot{q}) + g(q) = u, \tag{1}$$

where $q = (q_1, q_2, ..., q_n)^T$, $A(q)$ is an $(n \times n)$ positive definite inertia matrix, $b(q,\dot{q})$ is a vector of nonlinear centripetal terms, $g(q)$ is the vector for gravity terms, and u is the vector of joint actuator inputs, usually torques for revolute joints.

We are interested in studying this system for the under-actuated case with a specific arrangement of actuators and torsion springs at the joints. The properties of controllability and feedback linearizability are difficult to establish for an under-actuated system if the mass distribution within the system is arbitrary [14]. In our recent work [12], we had shown that certain choices of inertia distributions make an under-actuated open-chain planar robot with revolute joints feedback linearizable, i.e., also differentially flat. On similar lines, we choose the mass distribution in the following recursive way: (i) the center of mass of the last link n is on joint axis n, (ii) the center of mass of the last two links n and $n-1$ lies on the joint axis $n-1$, (iii) this procedure repeats until the center of mass of the last $n-1$ links, i.e., center of mass of links n, $n-1$,..,2 is on the second joint axis. One of the ways by which such an inertia distribution can be achieved is through counterbalancing. Since the inertially fixed joint represents the foot contact with ground, it is left passive. Last j joints such that $j \le n-1$ are actuated and rest of the joints i.e. joint 1 to joint $(n-j)$ are passive with torsional springs. The equations of motion of this system, with the given special inertia distribution in each leg, has the structure shown in (2), the superscript j signifies that in each leg, j terminal joints are actuated. For the assumed inertia distribution, it can be shown [12] that the inertia matrix becomes a constant $n \times n$ matrix and assumes a special reflected 'L' pattern. Since, inertia matrix becomes a constant, the coriolis terms go away. The n dimensional vector $g(q)$, corresponding to potential terms, is left with only one nonlinear term shown in (4).

$$A^j\ddot{q} + g^j(q_1) = u, \tag{2}$$

$$A^j = \begin{bmatrix} a_{11}^j & a_{22}^j & a_{33}^j & \$ & \% & \ldots & a_{nn}^j \\ a_{22}^j & a_{22}^j & a_{33}^j & \$ & \% & \ldots & a_{nn}^j \\ a_{33}^j & a_{33}^j & a_{33}^j & \$ & \% & \ldots & a_{nn}^j \\ \$ & \$ & \ldots & \$ & \% & \ldots & a_{nn}^j \\ \% & \% & \ldots & \% & \% & \ldots & a_{nn}^j \\ \vdots & \vdots & \vdots & \vdots & \vdots & \vdots & \vdots \\ a_{nn}^j & a_{nn}^j & \ldots & a_{nn}^j & a_{nn}^j & \ldots & a_{nn}^j \end{bmatrix} \tag{3}$$

$$g^j(q) = \begin{bmatrix} -2mgl\sin(q_1) \\ k_2 q_2 \\ \vdots \\ k_{n-j}q_{n-j} \\ 0 \\ \vdots \\ 0 \end{bmatrix}, u = \begin{bmatrix} 0 \\ 0 \\ \vdots \\ 0 \\ u_{n-j+1} \\ \vdots \\ u_n \end{bmatrix}. \tag{4}$$

Here, m is the mass of each leg as a whole.

A. *Feedback Linearizability of the Class of Bipeds*

If the system is fully actuated, all joint trajectories $q(t)$ are feasible. However, if the system is under-actuated, only those joint trajectories are valid that do not require inputs where the actuators are missing. The objective of this section is to investigate the property of *feedback linearizability* of bipeds, whose equations of motion have the structure of (2). The linearizing outputs are such that all output trajectories are feasible i.e. they satisfy the dynamics of the system.

The open-chain system described in Section II has $2n$ states, and potentially up to n inputs, if there is an actuator at every joint. For a fully actuated system, one can choose the n output functions simply as $y_i = q_i$, $i = 1, ...n$. Each of these output functions q_i can be shown to have relative degree 2 [9], [14]. As a result, the vector relative degree with these n output functions q_i is $2n$. This equals the dimension of the states $2n$ and the feedback linearizability of the fully-actuated system is established. However, if the system is under-actuated and has m inputs $(m < n)$, we are only allowed to choose m output functions that make up the vector relative degree $2n$.

In this paper, we study a particular choice of under-actuation for this system with special mass distribution in its last j bodies: A total of j joints starting from joint $n-j+1$ to joint n have actuators, while the remaining $n-j$ joints are passive but have torsional springs. With this choice, the vector u in (2) takes the special form $u = [0, ..., , u_{n-j+1}, .., u_n]^T$. This system is under-actuated by $n-j$, where $j \le n-1$. Note that j takes values from

1 to $n-1$. This covers a broad range of designs with the degree of under-actuation varying from 1 to $n-1$.

B. Flat Outputs with Full Relative Degree

In order to prove the feedback linearizability of this system, we choose j output functions and find their relative degrees. These output functions are selected as,

$$y = \begin{bmatrix} \sum_{i=1}^{n} a_{ii}^{j} q_i \\ a_{n-j+2\ n-j+2}^{j} (\sum_{i=1}^{n-j+2} q_i) + \sum_{i=n-j+3}^{n} a_{ii}^{j} q_i \\ \vdots \\ a_{nn}^{j} (\sum_{i=1}^{n} q_i) \end{bmatrix}, \quad (5)$$

where $y \in \mathcal{R}^j$. It should be noted that each flat output is a dot-product of a particular row of the inertia matrix in (3) with the configuration variable vector, $q = [q_1, q_2, ..., q_n]^T$. y_1 is a dot product of the first row of mass matrix with q, y_2 through y_j are dot products of q with rows $n-j+2$ through n of the inertia matrix, respectively. In order to find the relative degree of a particular output function, we differentiate this output until one or more inputs appear in the higher derivative of the output. For example, $\ddot{y}_j = a_{nn}^j (\sum_{i=1}^{n} \ddot{q}_i)$. From the last equation in (2)-(4), for $j \le n-1$, $\ddot{y}_j = a_{nn}^j (\sum_{i=1}^{n} \ddot{q}_i) = u_n$. Hence, the relative degree of j^{th} output is 2. Similarly, using the last $j-1$ of the dynamic equations (2)-(4), all flat outputs except the first have a relative degree of 2 making up a total relative degree of $2(j-1)$. For the system to be feedback linearizable/differentially flat, we need a total relative degree of $2n$, therefore, the first output y_1 has to have a relative degree of $2(n-j+1)$. On differentiating, $\ddot{y}_1 = \sum_{i=1}^{n} a_{ii}^j \ddot{q}_i$. From the structure of the first equation in (2)-(4),

$$\ddot{y}_1 = \sum_{i=1}^{n} a_{ii}^j \ddot{q}_i = 2mgl \sin(q_1). \quad (6)$$

Hence, the inputs do not appear in the second derivative $\ddot{y}_1$ and it must be differentiated further. On differentiating $\ddot{y}_1$ another two times, we get:

$$y_1^{(4)} = -2mgl(\sin(q_1)\dot{q}_1^2 - \cos(q_1)\ddot{q}_1). \quad (7)$$

For $j \ge n-2$, using the dynamical equations (2)-(4), $\ddot{q}_1$ can be solved explictly by subtracting the second equation from the first equation,

$$\ddot{q}_1 = [\frac{2mgl\sin(q_1) + k_2 q_2}{a_{11}^j - a_{22}^j}]. \quad (8)$$

and,

$$y_1^{(4)} = -2mgl \left(\sin(q_1)\dot{q}_1^2 - \cos(q_1)[\frac{2mgl\sin(q_1) + k_2 q_2}{a_{11}^j - a_{22}^j}] \right). \quad (9)$$

As a result, the inputs do not appear in the fourth derivative $y_1^{(4)}$. If $j = n-1$, using the above steps again, we get

$$y_1^{(4)} = -2mgl \left(\sin(q_1)\dot{q}_1^2 - \cos(q_1)[\frac{2mgl\sin(q_1) + u_2}{a_{11}^j - a_{22}^j}] \right). \quad (10)$$

Hence, for $j = n-1$, as required the relative degree of y_1 is $2(n-(n-1)+1) = 4$.

For the case with $j \ge n-2$, we differentiate (9) twice more and after substituting $\ddot{q}_1$ from (8) we find that $y_1^{(6)}$ has the following functional dependence:

$$y_1^{(6)} = f_6(q_1, \dot{q}_1, q_2, \dot{q}_2, \ddot{q}_2). \quad (11)$$

Two cases arise: (a) $j = n-2$, (b) $j \ge n-3$. For each of the two cases, $\ddot{q}_2$ can be obtained from the Dynamical Equations (2)-(4) by subtracting the third equation from the second equation and substituting $\ddot{q}_1$ from (8). For $j = n-2$, we get,

$$\ddot{q}_2 = [\frac{k_2 q_2 + u_3}{a_{33}^j - a_{22}^j}] - [\frac{2mgl\sin(q_1) + k_2 q_2}{a_{11}^j - a_{22}^j}]. \quad (12)$$

Substituting this in (13) we get,

$$y_1^{(6)} = f_6^{u_3}(q_1, \dot{q}_1, q_2, \dot{q}_2, u_3). \quad (13)$$

Input u_3 has explicitly appeared in $y_1^{(6)}$. Hence, the relative degree of y_1 is $6 = 2(n-j+1)$ for $j = n-2$, i.e. we have met the relative degree condition. For $j \ge n-3$, we get:

$$\ddot{q}_2 = [\frac{k_3 q_3 - k_2 q_2}{a_{22}^j - a_{33}^j}] - [\frac{2mgl\sin(q_1) + k_2 q_2}{a_{11}^j - a_{22}^j}]. \quad (14)$$

From (13) and (14), we can see that input has not appeared explicitly in $y_1^{(6)}$. We can continue this process until the input u_{n-j+1} appears in the highest derivative $y_1^{2(n-j+1)}$. Hence, it can be shown that the relative degree of the output function y_1 is $2(n-j+1)$. We have already shown in the beginning of this sub-section that each of the other output functions y_i, $i = 2, ..., j$ have a relative degree 2. As a result, the vector relative degree of the outputs y in (5) turns out to be $[2(n-j+1), 2, ..., 2, 2]$ and their sum equals the total number of states $2n$.

C. Existence of a Diffeomorphism

An additional property that must be shown with this feedback linearization is the existence of a diffeomorphism between the $2n$ states, j inputs and the j output functions and their derivatives. From (6), we see that $q_1 = \arcsin(\frac{\ddot{y}_1}{2mgl})$, so $\ddot{y}_1$ trajectory has to be chosen such that the argument of $it\arcsin(\cdot)$ is always less than unity. Differentiating (6) once and solving for $\dot{q}_1$ we get $\dot{q}_1 = \frac{y_1^{(3)}}{2mgl\cos(q_1)}$, we can substitute for q_1 here to get an explicit relationship. For $j = n-1$, subtracting the definitions of y_1 and y_2 from each other we get,

$$(a_{11} - a_{33})q_1 + (a_{22} - a_{33})q_2 = y_1 - y_2. \quad (15)$$

From here, q_2 can be computed by substituting for q_1. We can differentiate (15) and substitute $[q_1, \dot{q}_1]$ and compute $\dot{q}_2$.

Similarly we need to compute $y_1 - y_3$ for $[q_3, \dot{q}_3]$, ..., $y_1 - y_{n-1}$ for $[q_{n-1}, \dot{q}_{n-1}]$. Finally, we can use $[q_1, ..., q_{n-1}]$, $[\dot{q}_1, ..., \dot{q}_{n-1}]$ along with the definition of y_1 and its first derivative to compute $[q_n, \dot{q}_n]$. u_2 can be computed from (10) and $u_i = \ddot{y}_{i-1}, i = 3, ..., n$ from the last $n-2$ dynamic equations (2)-(4).

For $j = n-2$, expressions for $[q_1, \dot{q}_1]$ remain the same. $[q_2, \dot{q}_2]$ can be computed from (9) and its derivative by substituting for $[q_1, \dot{q}_1]$. Once $[q_1, q_2]$ and the corresponding rates are in place, $[q_i, \dot{q}_i]$ can be solved using expressions for $y_1 - y_{i-2}$ and its derivative. Again, $[q_n, \dot{q}_n]$ can be solved using the definition of $[y_1, \dot{y}_1]$ and expressions for $[q_1, ..., q_{n-1}]$ and $[\dot{q}_1, ..., \dot{q}_{n-1}]$. u_3 can be computed from (13) and $u_i = \ddot{y}_{i-2}, i = 4, ..., n$ from the last $n-3$ dynamic equations (2)-(4). These results can be generalized for cases with $j \leq n-1$.

III. PLANNING AND CONTROL

A system can follow any flat output trajectory because the state trajectories corresponding to any flat output trajectory, by definition, already satisfy the dynamic equations. Once the flat output and its diffeomorphism is established, any state of the system can be converted into a flat output space. A user can specify a set of such states that should be traversed by the robot. Using methods of collocation, flat output trajectories can be made to pass through a finite set of flat output states, making point to point manoeuvres possible. The nature of trajectories in between the specified states can be modulated to satisfy constraints, e.g. positive ground normal reaction for a biped robot. Numerical optimization has been used to select a trajectory from amongst a parameterized family of trajectories that satisfy all the motion constraints while optimizing a criterion. Following steps are followed to generate the family of trajectories: (i) First, we select a set of states and corresponding time instants and transform these states into flat outputs and their derivatives, (ii) Then, we form a polynomial function of time $(p_1(t))$ for flat outputs such that it goes through the required set of flat output states at given time instants. This set of states and time instants are also treated as parameters of optimization, (iii) Then, we form another polynomial $p_2(t)$ such that it gives zero flat output states at the specified time instant, (iv) Using these two polynomial functions we form the parameterized family of flat output trajectories as follows:

$$y(t) = p_1(t) + p_2(t)\left(\sum_{i=0}^{n} \left\{ a_i \cos\left(\frac{2i\pi t}{T}\right) + b_i \sin\left(\frac{2i\pi t}{T}\right) \right\}\right), \quad (16)$$

where T is the time separation between the first and last state in the chosen set of states. The coefficients (a_i, b_i), the set of states and corresponding time instants are all parameters of optimization. An objective function minimizing the sum of squares of torques integrated over the entire period of the gait is selected, (18). Once we have a feasible plan for the flat outputs, we design a tracker in the flat output space. First, we define a new set of states given by $v_i = y_i^{(r_i)}$, where

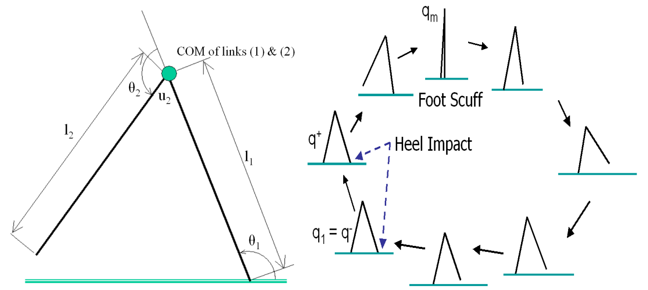

Fig. 2. (Left) A two DOF planar biped robot with no knee joint with only hip joint actuated. (Right) The gait of the two DOF biped. The stance leg and swing leg interchange their roles at the ground impact with a small foot scuffing near the vertical configuration of the biped.

$i = 1, ..., j$ and r_i denotes the relative degree of the i^{th} flat output. Each of the new control inputs are computed using (18).

$$f = \int_0^T u \cdot u \; dt. \quad (17)$$

$$v_i = y_d^{(r_i)} + k_1^i(y_d^{(r_i-1)} - y^{(r_i-1)}) + ... + k_{r_i}^i(y_d - y). \quad (18)$$

The subscript d in (18) denotes the planned trajectories. The actual inputs can be computed using the diffeomorphism having the functional form, $u_i = g_i(y_1, ..., y_1^{r_1}, y_2, ..., y_2^{(r_1)}, ..., y_j, ..., y_j^{(r_1)}), i = 1, ..., j$.

IV. TWO DOF BIPED

In this section, the methodology proposed is illustrated with a simple example of a two degree-of-freedom biped shown in Fig. 2. Both the legs are identical with the center-of-mass of each leg at the hip joint. This biped is under-actuated with only the hip joint actuated. At any given instance one of the legs (stance leg) is in contact with the ground and the other leg (swing leg) is swinging freely in air. The legs interchange their role instantenously when the swing leg hits the ground (ground impact). Following the terminology presented in the previous section, for this biped, $n = 2$ and $j = 1$, hence, this biped is under-actuated by $n - j = 1$.

A. Dynamic Model

The dynamical equations are derived using the Lagrangian and non-dimensionalized to give the following form.

$$\begin{bmatrix} 1 & \epsilon \\ \epsilon & \epsilon \end{bmatrix} \begin{bmatrix} \ddot{q}_1 \\ \ddot{q}_2 \end{bmatrix} = \begin{bmatrix} \sin(q_1) \\ u \end{bmatrix},$$

$$\epsilon = \frac{I}{2(I + ml^2)}, \tau = \frac{t}{\sqrt{\frac{I+ml^2}{mgl}}}, u = \frac{u_2}{2mgl}, \quad (19)$$

where the dots represent the derivative w.r.t to normalized time τ, u is a normalized input, m is the mass of each leg, l is the length of each leg, I is the moment of inertia of each leg about its center-of-mass, g is the acceleration due to gravity and u_2 is the input torque at the hip joint. The ground impact happens when the swing leg hits the ground, it happens when $2q_1 + q_2 = \pi$. The impact is instantaneous, during which the angular velocities change but the configuration is invariant. The impact model can be derived by using conserving angular momentum or energy methods with a standard procedure used in most of the walking literature [1].

B. Flat Outputs and Diffeomorphism

As described in Section II-A, flat output is chosen to be $y = y_1 + \epsilon y_2$. The diffeomorphism and input-output relation are given in (20). Clearly, for the diffeomorphism to be meaningful $|\ddot{y}| \leq 1$.

$$
\begin{aligned}
q_1 &= \arcsin \ddot{y}, \qquad q_2 = \frac{1}{\epsilon}(y - \arcsin(\ddot{y})), \\
\dot{q}_1 &= \frac{y^{(3)}}{\sqrt{1-\ddot{y}^2}}, \qquad \dot{q}_2 = \frac{1}{\epsilon}(\dot{y} - \frac{y^{(3)}}{\sqrt{1-\ddot{y}^2}}), \\
u &= \ddot{y} - \frac{1-\epsilon}{\sqrt{1-\ddot{y}}}\left[y^{(4)} + \frac{{y^{(3)}}^2 \ddot{y}}{1-\ddot{y}^2} \right].
\end{aligned} \tag{20}
$$

C. Planning and Control

The swing foot of the biped has to clear the ground at all times. Since, this is a two DOF biped there will be a small amount of foot scuffing near the vertical configuration of both the legs. We can minimize the amount of foot scuffing by constraining the state q_m in Fig. 2 at the beginning of foot scuffing to be as close to the vertical configuration as possible. If q^- represents the state of the system just before the impact, then the state of the system right after the impact q^+ can be determined from the impact model. Starting from a particlar q^- at time $t = 0$, the system goes through $q_m(t = t_m)$ and finally the impact happens at $q^-(t = T)$ where T is gait period. To ensure a limit cycle, the state at the end of the gait just before the impact q^- should be such that it transforms to the q^+ that the biped started off with. As described in Section III, we followed these steps to plan a trajectory. (i) First, a suitable q^- and a q_m close to a vertical position were selected, (ii) Then, using the impact model, a q^+ is generated using the chosen q^-, (iii) Then, all the three states $[q^+, q_m, q^-]$ were converted into the flat output states $[y^+, y_m, y^-]$ using (20), (iv) A class of flat output trajectories is generated in the form (16). $p_1(t) = \sum_{i=0}^{12} a_i t^i$ ensures that the flat output trajectories goes through the three flat output states at their respective time instants. $p_2(t) = (t-T)^4(t-t_m)^4 t^4$ is homogeneous at the three time instants, ensuring that the Fourier series chosen to modulate the trajectories does not affect the three flat output states.

Once we have the parameterized trajectory the planning problem can be formulated as an optimization problem to minimize (18). The parameters of optimization $a_i, b_i, q^-, q_m, t_m, T$. q^-, q_m are chosen such that the condition $2q_1 + q_2 = \pi$ for both feet on ground is satisfied and the angular velocities have a correct direction. The constraints

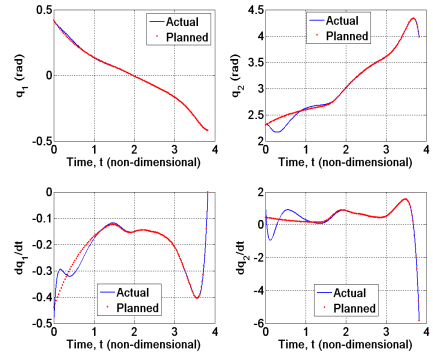

Fig. 3. Planned trajectories and tracking results for the two DOF biped. With initial errors the system eventually converges to the planned trajectories.

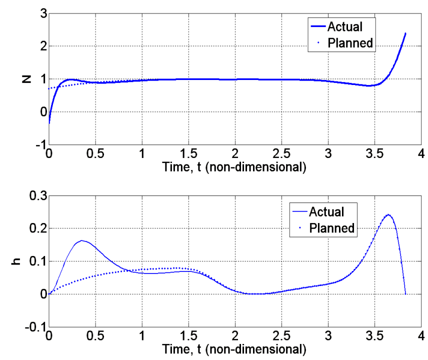

Fig. 4. The planned and actual ground normal reaction (N) and heel height (h). The qualifier "actual" implies the quantities for the system with initial errors. Both normal reaction and heel height have to be positive.

imposed during optimization are:

$$
\begin{aligned}
T \quad &\leq \quad T_{max}, \qquad && |\ddot{y}| \leq 1, \\
-\frac{pi}{4} < \quad & q_1^- \quad < 0, && \dot{q}_1 < 0, \\
N \quad &> \quad 0, && h > 0, \\
-0.08 \quad & < q_{m1} < 0.08. &&
\end{aligned} \tag{21}
$$

The first constraint keeps the gait period in bounded. The second constraint is necessary for the diffeomorphism to exist. The third constraint ensures a reasonable initial state of the biped. The fourth constraint makes sure that the biped always moves forward. The fifth and sixth inequalities constrains the ground normal reaction N and heel height to be positive, respectively.The last constraint makes sure that the foot scuff happens in a nearly vertical configuration. As described in section III, a new input is defined as $v = y^{(4)}$. The equations for the real input and the feedback control law are as follows:

$$
u = \ddot{y} - \frac{1-\epsilon}{\sqrt{1-\ddot{y}}}\left[v + \frac{{y^{(3)}}^2 \ddot{y}}{1-\ddot{y}^2} \right]. \tag{22}
$$

$$
v = y_d^{(4)} + k_1(y_d^{(3)} - y^{(3)}) + ... + k_4^i(y_d - y). \tag{23}
$$

D. Simulation Results

Planning and simulations for control were carried out for $\epsilon = 0.07$ based on the parameters of a design presented

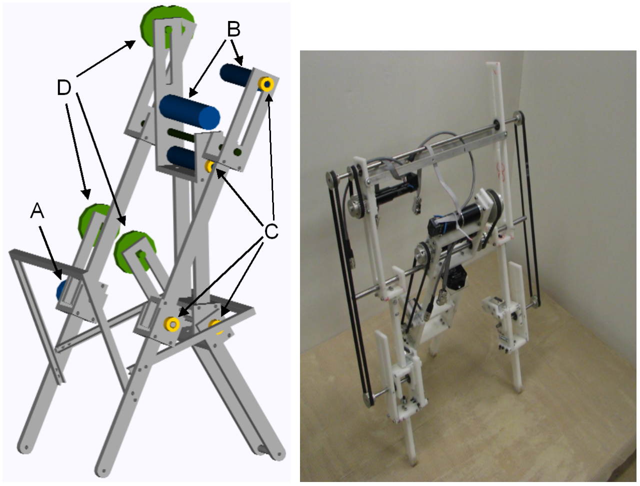

Fig. 5. A four link biped having a shank and a thigh in each leg. The knee joint has a stopper to avoid hyper-extension and there are latches (A) that lock the knee joint after the knee impact. Maxon motors (B) are placed at the hip and they drive the corresponding axis via a pulley (C) and belt arrangement. Counterweights (D) are used to place the center of mass at the respective joints.

in the next section. The feedback gains in (23) were taken to be $[k_1, k_2, k_3, k_4] = [18, 119, 400, 500]$. The constraints presented in the previous section were imposed at fixed number of time instants during the gait. Once a plan was generated by numerical optimization, the validity of constraints was verified for the entire gait. The cost function was also evaluated by summing the square of input at fixed number of time instants. An SQP based numerical optimization routine $fmincon^{©}$ from $Mathworks$ was employed for the optimization. Fig. 3 presents the planning and tracking results for the biped. We can see that even with errors in initial conditions the system eventually converges to the planned trajectories. The normal reaction and heel height in Fig. 4 stay positive over a period of the gait.

V. A DESIGN OF THE BIPED

A four link planar biped has been fabricated for experiments, shown in Fig. (5). The lateral stability problem is avoided by using a crutch type design, where each leg comprises of two widely spaced chain of links constrained to move rigidly. Each of the two legs has a shank and a thigh with a revolute knee joint and the hip joint. The knee joints have a rigid stopper that avoids hyper-extension and there are latches at both knee joints that lock the knee joint in place after the knee impact. The motors are placed near the hip reducing the counterweights required for center of mass placement. Inclinometers are used to measure the absolute orientation of the legs. With the knee joints locked, this biped can be controlled as two degree-of-freedom biped simulated in the previous section. The foot scuffing with only two degrees-of-freedom can be avoided by using a pattern of alternate tiles on the ground. This biped is $54cms$ in height, weighs around $9kg$.

VI. CONCLUSIONS

The property of *differential flatness* for a class of an n-DOF under-actuated planar bipeds and its dependence on inertia distribution within the system has been studied. It has been shown that certain choices of inertia distributions make an under-actuated planar biped with revolute joints feedback linearizable, i.e., also differentially flat. Once this property is established, trajectory between any two points in its differentially flat output space is feasible and can be shown to be consistent with the dynamics of the under-actuated system. This enables the under-actuated system to follow both cyclic as well as point to point trajectories. The entire methodology is illustrated by applying it to a two DOF planar under-actuated bipeds. Planning and tracking results from simulations were presented for the same. We are currently in the process of setting up an experiment to validate the ideas presented. In future, we will study issues of energetics and robustness of the proposed design.

VII. ACKNOWLEDGMENTS

We sincerely thank Dr. Jaume Franch for discussions related to this work.

REFERENCES

[1] T. McGeer, "Passive Dynamic Walking", *International Journal of Robotics Research*, vol. 9, n 2, 1990, pp. 62-82.

[2] S. H. Collins, M. Wisse, and A. Ruina, A three-dimensional passive-dynamic walking robot with two legs and knees, *International Journal of Robotics Research*, vol. 20, n 7, 2001, pp. 607615.

[3] K. Hirai, M. Hirose, Y. Haikawa and T. Takenaka, "The Development of the Honda Humanoid Robot", *Proceedings of IEEE International Conference on Robotics and Automation*, 1998, pp. 1321-1326.

[4] H. Inoue, S. Tachi, Y. Nakamura, N. Ohyu, S. Hirai, K. Tanie, K. Yokoi and H. Hirukawa, "Overview of Humanoid Robotics Project of METI", *Proceedings of the 32nd ISR*, 2001.

[5] J. W. Grizzle, G. Abba and F Plestan, "Asymptotically Stable Walking for Biped Robots: Analysis via Systems with Impulse Effect", *IEEE Transactions on Automatic Control*, vol. 46, n 1, 2001, pp. 51-64.

[6] J. W. Grizzle and C. H. Moog, "Nonlinear Control of Mechanical Systems with an Unactuated Cyclic Variable", *IEEE Transactions on Automatic Control*, vol. 50, n 5, 2005, pp. 559-576.

[7] L. Cambrini, C. Chevallereau, C. H. Moog and R. Stojic, "Stable Trajectory Tracking for Biped Robots", *Proceedings of the 39th IEEE Conference on Decision and Control*, 2000, pp. 4815-4820.

[8] A. Chemori and A. Loria, "Control of a Planar Underactuated Biped on a Complete Walking Cycle", *IEEE Transactions on Automatic Control*, vol. 49, n 5, 2004, pp. 838-842.

[9] H. Sira-Ramirez and S. K. Agrawal, *Differentially Flat Systems*, Marcel Dekker, Inc., New York, Basel, 2004.

[10] N. Faiz, S. K. Agrawal and R. M. Murray, "Trajectory Planning of Differentially Flat Systems with Dynamics and Inequalities", *AIAA Journal of Guidance, Control, and Dynamics*, vol. 24, n 2, 2001, pp. 219-227.

[11] P. Tsiotras and J. Luo, "Control of under actuated spacecraft with bounded inputs", *Automatica*, vol. 36, n 8, 2000, pp. 1153-1169.

[12] S. K. Agrawal and V. Sangwan, "Design of Under-Actuated Open-Chain Planar Robots for Repetitive Cyclic Motions", *Proceedings of ASME 2006 International Design Engineering Technical Conferences*, 2006.

[13] M. W. Spong, M. Vidyasagar, *Robot Dynamics and Control*, John Wiley & Sons, 1989.

[14] A. Isidori, *Nonlinear Control Systems*, Communications and Control Engineering, Springer, III edition , 1995.